LUNAR FORMATION

Dating the Moon-forming impact event with asteroidal meteorites

W. F. Bottke,[1]* D. Vokrouhlický,[2] S. Marchi,[1] T. Swindle,[3,4] E. R. D. Scott,[5] J. R. Weirich,[6] H. Levison[1]

The inner solar system's biggest and most recent known collision was the Moon-forming giant impact between a large protoplanet and proto-Earth. Not only did it create a disk near Earth that formed the Moon, it also ejected several percent of an Earth mass out of the Earth-Moon system. Here, we argue that numerous kilometer-sized ejecta fragments from that event struck main-belt asteroids at velocities exceeding 10 kilometers per second, enough to heat and degas target rock. Such impacts produce ~1000 times more highly heated material by volume than do typical main belt collisions at ~5 kilometers per second. By modeling their temporal evolution, and fitting the results to ancient impact heating signatures in stony meteorites, we infer that the Moon formed ~4.47 billion years ago, which is in agreement with previous estimates.

Insights into the last stages of terrestrial planet formation can be gleaned from the abundances and chondritic signatures of highly siderophile elements (HSEs) (such as Re, Os, Ir, Ru, Pt, Rh, Pd, and Au) found in the mantles of Earth and the Moon (*1*). Consider that the "giant impact" (GI) that formed the Moon probably sent all HSEs in Earth and the Moon to their respective metallic cores. If true, HSEs measured in the terrestrial and lunar mantles today were added late, with ~0.5 and ~0.02% of the planetary masses of Earth and the Moon, respectively, delivered by ancient chondritic projectiles after the GI (*1*). These low values imply that the GI took place near the endgame of planet formation. In addition, the ratio of accreted mass on Earth compared with the Moon, ~700 to 1200, is also curious; this value is much larger than the ratio of the gravitational crosssections of Earth and the Moon, ~20 (*1*, *2*). This difference can be explained if terrestrial and lunar HSEs were delivered by a few very large bodies rather than numerous small bodies (*1*). A key additional implication, however, is that the number of small leftover planetesimals in the inner solar system at the time of the GI was also likely to be limited.

Taken together, these inferences open the door for GI ejecta to dominate the population of kilometer-sized bodies in the terrestrial planet region during the late stages of planet formation. As evidence, consider that GI simulations, capable of reproducing Earth-Moon system constraints, often eject several percent of an Earth mass out of Earth's gravitational sphere of influence (*3*–*5*). If a considerable fraction of this mass were solid debris, as described by many GI simulations (*3*–*5*), and the GI ejecta size frequency distribution had a steep slope, which we infer from modeling work (*6*) and data (*7*), numerous kilometer-sized bodies could plausibly have struck main-belt asteroids at velocities $V > 10$ km/s (Fig. 1) (*8*). Impact heating here is accentuated, with numerical hydrocode impact experiments showing that the volume of target material obtaining a ^{40}Ar-^{39}Ar shock degassing age (*8*–*11*) at $V > 10$ km/s is nearly three orders of magnitude higher than at typical main-belt collision velocities of ~5 km/s (*8*, *12*). Moreover, these velocities are only obtained by projectiles on highly eccentric and/or inclined orbits, such as leftover planetesimals (*13*) or GI ejecta (Fig. 1) (*14*). Thus, a record of ancient GI ejecta impact events could be observable in stony meteorites.

To test this possibility, we constructed models of ^{40}Ar-^{39}Ar reset age profiles for stony meteorites that included contributions from both leftover planetesimals and GI ejecta. Our results were then compared with ^{40}Ar-^{39}Ar ages for chondrites derived from large collisions between 4.35 to 4.567 billion years ago (Ga) (Fig. 2A) (*9*–*11*). The older age is that of the calcium-aluminum–rich inclusions (CAIs), the first-formed solids (*15*). The younger age marks the start of a relative lull in ^{40}Ar-^{39}Ar reset ages; few are found between ~4.1 and 4.4 Ga, whereas many exist between 3.5 to 4.1 Ga, the time of the late heavy bombardment (*8*–*10*, *12*). Our goal is to deduce both the timing of the GI and the relative magnitude of the bombardment by GI ejecta and that by leftover planetesimals.

The evidence that the GI ejecta size frequency distribution was steep enough to produce a large number of kilometer-sized fragments can be inferred in part from the ancient lunar impact record. Using numerical simulations to track GI ejecta, and assuming that the bodies were not strongly affected by collisional evolution or nongravitational dynamical forces, we found that

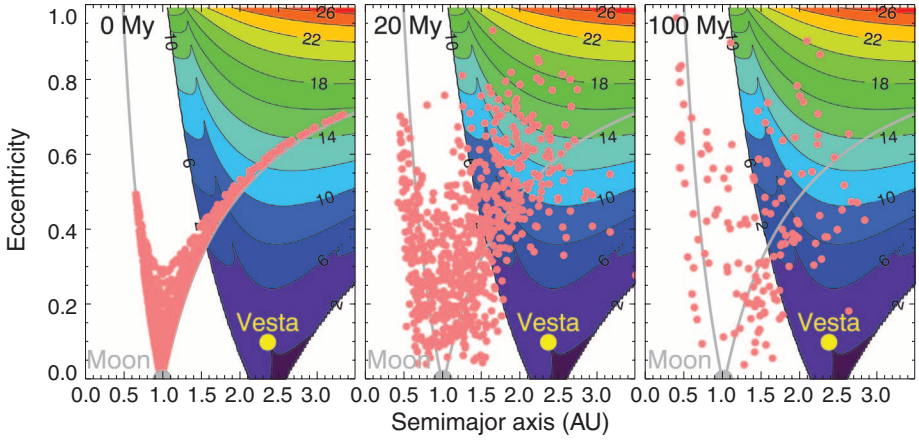

Fig. 1. The dynamical evolution of GI ejecta. Here, we show a sample of our 30,000 test bodies, all which were tracked for 600 My by using the numerical integrator SWIFT-RMVS3 (*29*). The planets Venus through Neptune were included in the integrations, with orbits as described in (*17*). The initial orbits of the ejecta test bodies were defined by placing them on Earth's Hill sphere, with a random isotropic trajectory away from Earth's center. They were then assigned an initial ejection velocity "at infinity" of 1, 3, 5, 7, or 9 km/s, respectively. These results were used to calculate impact frequencies on the Moon and terrestrial planets as well as the collision probability and impact velocity distributions between our test bodies and our representative main-belt target asteroid Vesta (*8*). Our results were combined by setting the initial velocity distribution of GI ejecta to values corresponding to GI hydrocode simulations; 14, 27, 26, 18, and 15% of the objects were assumed to be ejected at 1, 3, 5, 7, and 9 km/s, respectively (*14*). A sample of 1000 test bodies that use these velocity values are shown at several evolution times after the GI, with 38 and 6.5% left at 20 and 100 My, respectively. The color contours show the collision velocities of objects with Vesta in kilometers per second if their inclinations were 10° (*12*, *23*).

[1]Southwest Research Institute and NASA Solar System Exploration Research Virtual Institute (SSERVI)–Institute for the Science of Exploration Targets (ISET), Boulder, CO, USA. [2]Institute of Astronomy, Charles University, V Holešovičkách 2, CZ-18000, Prague 8, Czech Republic. [3]Lunar and Planetary Laboratory, University of Arizona, Tucson, AZ, USA. [4]SSERVI Center for Lunar Science Exploration, Houston, TX, USA. [5]Hawai'i Institute of Geophysics and Planetology, University of Hawai'i at Manoa, Honolulu, Hawai'i 96822, USA. [6]Department of Earth Sciences, Western University, London, ON, Canada.
*Corresponding author. E-mail: bottke@boulder.swri.edu

~1% come back to strike the Moon within 400 million years (My) (Fig. 1) (*8*). Because the Moon only has ~25 ancient (Pre-Nectarian) lunar basins (*16*), probably made by the impact of diameter D > 20 km projectiles >4.1 Ga (*13*, *17*), an impact probability of ~1% implies the GI ejecta population could—at best—only contain a few thousand D > 20 km bodies (the order of 25/0.01). Mass balance therefore requires the majority of GI ejecta to be in a steep size frequency distribution dominated by D < 20 km bodies (*8*). This leads us to predict that ~10^{10}-km-sized projectiles were thrown out of the Earth-Moon system (fig. S8) (*8*).

Although GI simulations lack the resolution to confirm the nature of this steep size frequency distribution, insights gleaned from numerical impact experiments on D = 100 km bodies show that such steep slopes are common outcomes when the targets are largely left intact (*6*). An analog in nature for this may be the formation of the ~500-km Rheasilvia basin on the D = 530 km asteroid Vesta; the largest body in Vesta's family of fragments is D ~ 8 km, a factor of 70 smaller than Vesta itself, whereas the exponents of its cumulative power law size distribution are extremely steep, with −3.7 and −8 observed for D > 3 km and > 5 km bodies, respectively (fig. S6) (*7*, *8*, *18*). The shape of this size distribution implies that much of the mass of GI ejecta was initially in the form of 0.1 < D < 20 km fragments rather than of dust and small debris (*8*).

A consequence of a steep GI ejecta size frequency distribution is that the fragments should undergo vigorous collisional evolution with themselves. Tests using collision evolution codes (*13*, *19*) indicate that D < 1 km bodies rapidly demolished themselves, enough so to reduce the population by several orders of magnitude in mass within 0.1 to 1 My of the GI (fig. S8) (*8*). This would lead to a huge dust spike, with small particles either thrown out of the solar system via radiation pressure or lost to the Sun via Poynting-Robertson drag (*14*, *20*). The surviving fragments were depleted enough that they settled into a quasi-collisional steady state, with subsequent mass loss dominated by dynamical processes. The net effect is that ~10^5 to 10^7 D > 1 km bodies were left in the GI ejecta population for many tens of millions of years (fig. S8).

A substantial fraction of GI ejecta reached asteroid belt–crossing orbits after the GI, either by being launched onto such orbits or by dynamically evolving there via planetary perturbations and resonances (Fig. 1 and fig. S1). We explored their impact consequences for large main-belt asteroids by calculating how they affected a representative main belt target, Vesta. Vesta was chosen because it is a likely source of the eucrite meteorites (*21*), Vesta's fragments have access to the gravitational resonances thought to provide most meteorites to Earth (*22*), and its eccentricity and inclination are close to average main-belt values (*23*). By calculating collision probability and impact velocity distributions over time between GI ejecta and Vesta (fig. S2) (*8*, *23*), we found that many fragments should have hit

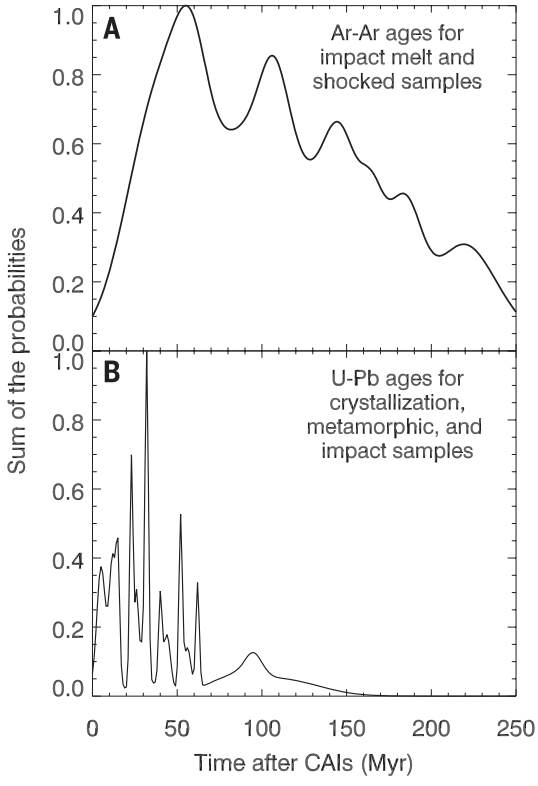

Fig. 2. Compilations of impact ages found within chondritic meteorites. (**A**) A representation of ^{40}Ar-^{39}Ar shock degassing ages for 34 ordinary and enstatite chondrites whose mean ages are between ~4.32 billion and 4.567 billion years (*9*–*11*). All samples were heavily shocked, shock-melted, or otherwise had some evidence for having been part of a large collision. To create this age-probability distribution, we separated the sample ages by parent body (EL, EH, E-melt/Aubrites, L, LL, and H chondrites) and computed the sum probability of ages within each class by adding Gaussian profiles, with centers and widths corresponding to the most probable age and 1σ errors of each dated sample (*8*). The profiles were then normalized before they were summed in order to prevent any single class from dominating the distribution (fig. S9A). We caution that systematic errors in measured Ar decay rates could make these ages slightly older (*8*). (**B**) The age-probability distribution of U-Pb ages for 24 L, LL, and H chondrites (table S1) created by using the same method (fig. S9B). U-Pb ages >60 My after CAIs are interpreted to be from impact heating alone, whereas those <60 My after CAIs are an unknown mixture of formation, metamorphic, and impact ages (*26*). Both distributions show a feature ~80 to 120 My after CAIs (~4.45 to 4.49 Ga).

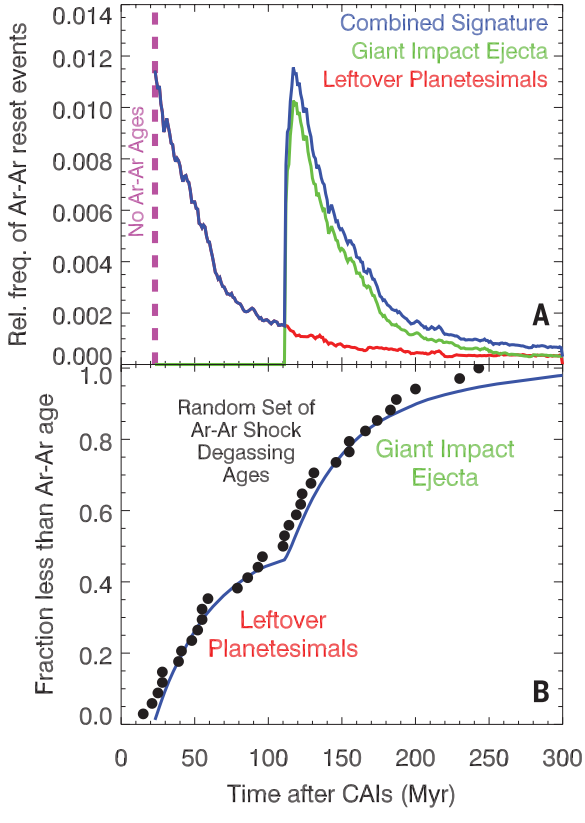

Fig. 3. A sample comparison between our model and randomly derived ^{40}Ar-^{39}Ar shock degassing ages for asteroidal meteorites. (**A**) The combined ^{40}Ar-^{39}Ar age distribution, in blue, was created by assuming that leftover planetesimals and giant impact ejecta struck main belt asteroids such as Vesta early in solar system history (*8*). Both model contributions have the same shape, with the former (red) ~1.8 times as large as the latter (green), respectively. (**B**) A single representation of our model results, shown as a blue line, compared with 34 ^{40}Ar-^{39}Ar shock reset ages randomly drawn from Fig. 2A. In this example, the giant impact takes place at 112 My after CAIs. The plotted results are close to our derived age for the giant impact, 105 ± 25 My after CAIs (equivalently 4.46 ± 0.03 Ga), and our derived contribution ratio of 1.9 ± 0.9 between leftover planetesimals and giant impact ejecta.

large main-belt asteroids. Two types of meteorite impact signatures were likely produced.

The first signature involves numerous kilometer-sized and smaller projectiles hitting Vesta and other very large asteroids ~0.1 to a few My after the GI. Many tens of $D > 10$ km craters and numerous smaller craters were potentially produced on Vesta during this interval. Their primary effect would have been to dredge up warm material heated at depth by early parent body metamorphism. This suddenly quenched material would have yielded a spike of impact ages from this time, with many samples showing little or modest shock effects. The second signature comes from impact heating within a crater's breccia lens or ejecta blanket, which would have been dominated by $V > 10$ km/s projectiles (Fig. 1). This mechanism should have produced ^{40}Ar-^{39}Ar shock reset ages on the target bodies for ~100 My after the GI. Subsequent impacts, such as the ~1-billion-year-old Rheasilvia basin formation event, excavated some of this material and placed it off-world, where collisions, nongravitational forces, gravitational resonances, and planetary encounters delivered it to Earth (*24*). Additional isotopic chronometers may also record these impacts (such as U-Pb), although this may involve higher-threshold temperatures and different heating durations than for Ar.

For our model ^{40}Ar-^{39}Ar reset age profiles created by GI ejecta, we combined these collisional and dynamical outcomes with impact heating relationships derived in (*8*, *12*) (fig. S4). The GI ejecta age profile was found to peak ~8 My after the GI, before slowly fading over the subsequent ~100 My (Fig. 3A and fig. S5). The leftover planetesimal ^{40}Ar-^{39}Ar reset age profile was more complicated to assess, mainly because existing planet formation models are uncertain and incomplete. As a compromise, we took advantage of insights from (*13*) that show that leftover planetesimal populations quickly decimate themselves through collisional evolution. The survivors, left in a quasi–steady state with limited mass in small bodies, are then slowly lost from high eccentricity and inclination orbits over time. Although our tests with different starting size distributions and dynamical populations yielded a range of ^{40}Ar-^{39}Ar reset age profiles, the tails of the age profiles showed shapes similar to those computed for GI ejecta. These profiles, when scaled appropriately, also provided an excellent fit to our oldest ^{40}Ar-^{39}Ar data (Fig. 3B). We therefore assumed for simplicity that the shape of the leftover planetesimals' reset age profile tail mimicked that found for GI ejecta.

Our model results were compared with a representation of ancient ^{40}Ar-^{39}Ar shock degassing ages from 34 chondritic samples derived from at least five or six asteroid parent bodies (Fig. 2A and fig. S9) (*8*–*11*). Using a Monte Carlo method, we randomly selected sample ages from an age-probability distribution (Fig. 2A and fig. 3B) and used a Kolmogorov–Smirnov test (K-S) statistical test to determine the quality of fit between model and data over 1000 trials. In each trial, we tested all possible combinations of our model GI ages, varied between 0 and 300 My after CAIs, and the ratio of the contributions of the reset age profiles of leftover planetesimals to that of GI ejecta varied between 0.01 and 100. The leftover planetesimal reset age profile was defined as starting from 0 My after CAIs, whereas the GI ejecta reset age profile was started at the model GI age. The two profiles were then scaled, added, and then compared against the sample data. By collecting and analyzing the high goodness of fit cases, we estimate that the GI took place 105 ± 25 My after CAIs (equivalently 4.46 ± 0.03 Ga, 1σ confidence limits). The ratio of the leftover planetesimal contribution to that of giant impact ejecta was 1.9 ± 0.9.

Although this solution is promising, insufficient data exist to statistically argue it is unique. For this reason, we examined additional data sets for evidence that our inferred GI age was reasonable. Among the eucrite meteorites, there is a spike of ^{40}Ar-^{39}Ar ages between 4.47 and 4.49 Ga from at least nine unbrecciated samples (fig. S10) (*8*, *9*, *12*, *25*). They are interpreted to be impact by products, and their nature corresponds well to our GI quench age predictions. Similarly, a compilation of chondrite U-Pb ages (table S1) shows a prominent feature ~95 My after CAIs (~4.47 Ga) (Fig. 2B) that appears comparable with a ^{40}Ar-^{39}Ar shock degassing age feature at ~106 My after CAIs (~4.46 Ga) (Fig. 2A). We cannot yet apply our model to U-Pb data, however, because only the U-Pb ages >60 My after CAIs are considered to have been solely created by impact (*26*).

The intersection of these ages indicates that the likely timing of the giant impact was ~4.47 Ga. This value is a good match to the oldest lunar crust ages as well as several predicted ages found by other means (fig. S11) (*8*). It also indicates that the interval between the GI and the oldest collectable lunar samples was relatively short.

These results also offer the appealing possibility that remnants of GI ejecta—perhaps in the form of clasts with compositions akin to the crust, mantle, or core expected from the proto-Earth or the Moon-forming impactor—might be identified within ancient asteroid meteorite breccias. They also suggest that the GI was the most recent impact event of this scale in the terrestrial planet region. Other putative large-impact events, such as those taking place on early Earth or Venus, probably had to occur within the first few tens of millions of years after CAI formation, when their impact signatures could be most easily hidden among the ^{40}Ar-^{39}Ar ages provided by leftover planetesimals. Alternatively, these collisions, or comparatively smaller ones such as the putative impact event that produced Mars's ancient Borealis basin (*27*), either produced too little kilometer-sized ejecta fragments to be noticed in the available data or they occurred so close in time to the GI that the signature of their ejecta cannot yet be distinctly distinguished (*28*). Last, although the importance of GI ejecta returning to strike the Moon has yet to be quantitatively evaluated, the values computed here suggest that it could play an intriguing role in the earliest phase of lunar bombardment.

REFERENCES AND NOTES

1. W. F. Bottke, R. J. Walker, J. M. D. Day, D. Nesvorný, L. Elkins-Tanton, *Science* **330**, 1527–1530 (2010).
2. S. Marchi *et al*., *Nature* **511**, 578–582 (2014).
3. R. M. Canup, *Icarus* **196**, 518–538 (2008).
4. M. Ćuk, S. T. Stewart, *Science* **338**, 1047–1052 (2012).
5. R. M. Canup, *Science* **338**, 1052–1055 (2012).
6. D. D. Durda *et al*., *Icarus* **186**, 498–516 (2007).
7. D. Nesvorný, Nesvorný HCM Asteroid Families V2.0 NASA Planetary Data System, (2012).
8. Materials and methods are available as supplementary materials on *Science* Online.
9. D. D. Bogard, *Chem. Erde Geochem.* **71**, 207–226 (2011).
10. T. D. Swindle, D. A. Kring, J. R. Wierich, *Advances in 40Ar/39Ar Dating: from Archeaology to Planetary Sciences*, Geological Society of London, Special Publications, **378**, 333–347 (2013).
11. J. Hopp, M. Trieloff, U. Ott, E. V. Korochantseva, A. I. Buykin, *Meteorit. Planet. Sci.* **49**, 358–372 (2014).
12. S. Marchi *et al*., *Nat. Geosci.* **6**, 303–307 (2013).
13. W. F. Bottke, H. F. Levison, D. Nesvorný, L. Dones, *Icarus* **190**, 203–223 (2007).
14. A. P. Jackson, M. C. Wyatt, *Mon. Not. R. Astron. Soc.* **425**, 657–679 (2012).
15. J. N. Connelly *et al*., *Science* **338**, 651–655 (2012).
16. D. E. Wilhelms, *U.S. Geol. Surv. Prof. Pap.*, paper 1348 (1987).
17. W. F. Bottke *et al*., *Nature* **485**, 78–81 (2012).
18. P. Schenk *et al*., *Science* **336**, 694–697 (2012).
19. A. Morbidelli, W. F. Bottke, D. Nesvorný, H. F. Levison, *Icarus* **204**, 558–573 (2009).
20. J. A. Burns, P. L. Lamy, S. Soter, *Icarus* **40**, 1–48 (1979).
21. H. Y. McSween Jr. *et al*., *Meteorit. Planet. Sci.* **48**, 2090–2104 (2013).
22. A. Morbidelli, B. Gladman, *Meteorit. Planet. Sci.* **33**, 999–1016 (1998).
23. W. F. Bottke, M. C. Nolan, R. Greenberg, R. A. Kolvoord, *Icarus* **107**, 255–268 (1994).
24. W. F. Bottke Jr., D. Vokrouhlický, D. P. Rubincam, D. Nesvorný, *Annu. Rev. Earth Planet. Sci.* **34**, 157–191 (2006).
25. T. Kennedy, F. Jourdan, A. W. R. Bevan, M. A. Mary Gee, A. Frew, *Geochim. Cosmochim. Acta* **115**, 162–182 (2013).
26. R. H. Jones *et al*., *Geochim. Cosmochim. Acta* **132**, 120–140 (2014).
27. M. M. Marinova, O. Aharonson, E. Asphaug, *Nature* **453**, 1216–1219 (2008).
28. F. Nimmo, S. D. Hart, D. G. Korycansky, C. B. Agnor, *Nature* **453**, 1220–1223 (2008).
29. H. F. Levison, M. J. Duncan, *Icarus* **108**, 18–36 (1994).

ACKNOWLEDGMENTS

We thank R. Canup, B. Cohen, A. Jackson, A. Parker, P. Renne, and J. Salmon for many useful discussions and our referees for their numerous constructive comments. W.F.B, S.M., and T.S.'s participation was supported by NASA's SSERVI program through institute grant numbers NNA14AB03A and NNA14AB07A. The work of D.V. was partially supported by research grant P209-13-01308S of the Czech Grant Agency. Resources supporting this work were provided by the NASA High-End Computing Program through the NASA Advanced Supercomputing Division at Ames Research Center. Data are available in the main text, supplementary materials, or upon request.

SUPPLEMENTARY MATERIALS

www.sciencemag.org/content/348/6232/321/suppl/DC1
Materials and Methods
Figs. S1 to S11
Table S1
References (*30*–*70*)

10 October 2014; accepted 9 March 2015
10.1126/science.aaa0602

Dating the Moon-forming impact event with asteroidal meteorites

W. F. Bottke *et al.*

Science **348**, 321 (2015);
DOI: 10.1126/science.aaa0602